

Design, Synthesis of Nitrogen-Rich Triazine Derivatives and its Application in Water Sample, Vegetables and Oil Product

Xuelin Ma^{a,b}, Xiaoyong Zhang^b, Zhanzhong Hao^b, Limin Han^{a,*}

^a Chemical Engineering College, Inner Mongolia University of Technology, Hohhot 010051, P. R. China

^b Department of Chemistry, Baotou Teachers' College, Baotou 014030, P. R. China

Abstract A triazine nitrogen-rich derivative fluorescent probe, 1,1'-(6-chloro-1,3,5-triazine-2,4-diyl)bis(1H-benzo[d][1,2,3]triazole)(**L**), has been synthesized and successfully achieved for the efficient detection for Fe³⁺, Cr₂O₇²⁻, nitrobenzene as a turn-off chemosensor in DMF/H₂O. The quenching constant(K_{sv}) and detection of limit for Fe³⁺, Cr₂O₇²⁻, nitrobenzene on fluorescence response of the sensor can be as low as 470.00 M⁻¹, 359.94 M⁻¹, 3.62*10³ mL⁻¹, 2.10*10⁻⁵ M, 5.73*10⁻⁵ M, 1.24*10⁻⁵ mL, respectively. On the contrary, It is applied to detected for toluene and xylene as a turn-on chemosensor in DMF. The quenching constant and detection of limit for toluene and xylene on fluorescence response of the sensor can be as low as -11.05 mL⁻¹, -6.23 mL⁻¹, 9.30*10⁻⁴ mL, 7.35*10⁻³ mL, respectively. The application of water sample and vegetables showed that the **L** had high sensitive detection for Fe³⁺ ions. Meanwhile the application of gasoline, diesel and engine oil showed that the **L** had high sensitive detection for toluene and xylene.

Keywords: Triazine nitrogen-rich derivative; Multiple fluorescence sensor; Fe³⁺, Cr₂O₇²⁻ ions; Toluene, xylene and nitrobenzene

1 | INTRODUCTION

Environmental pollution has become an urgent global concern and the detection of toxic contaminants present in water has attracted significant research attention, it is very significant to effectively identify and remove the remaining pollutants from wastewater^[1]. There are lots of ways for water pollution, the most common is heavy-metal pollution. Heavy metal ions in natural water can easily enter the body of living organisms and animals. Ultimately, accumulation of heavy metals in the body of animals induces various diseases^[2]. The fluctuation of Fe³⁺ concentration also concerns with many health problems, including anemia, diabetes, even cancer. Therefore, Fe³⁺ detection is in great need due to the identification and diagnosis of the related diseases^[3]. The

* Corresponding author. E-mail address: hanlimin@imut.edu.cn (L. M. Han)

28 hexavalent chromate anions ($\text{Cr}_2\text{O}_7^{2-}$) in aqueous solution are highly carcinogenic to human and
29 harmful to living conditions, even with a relative low concentration^[4-7]. Upon skin contact, $\text{Cr}_2\text{O}_7^{2-}$
30 can cause genetic defects and allergic reactions^[8]. World Health Organization has identified these
31 ions as a Group “A” carcinogen^[9]. Aromatic compounds are also a source of water pollution,
32 especially toluene, xylene and nitrobenzene. These volatile toxic organic compounds can cause
33 irritation symptoms in the respiratory tract, skin, eyes, and cause fatigue, headache and dizziness,
34 and serious health problems such as heart arrhythmia, central nervous system disorders, and so on<sup>[10-
35 12]</sup>.

36 Up to the present, the detection methods cover electrochemical atomic absorption/emission
37 spectroscopy, voltammetry, inductively coupled plasma mass spectrometry, and potentiometry and
38 inductively coupled plasma mass spectrometry^[13-15]. However, above methods require sophisticated
39 instrumentation, complicated samples preparation, expensive reagents, time-consuming,
40 cumbersome pre-treatments such as solvent extraction, solid-phase extraction as well as
41 precipitation in order to achieve higher sensitivity. Fortunately, fluorescent probes have attracted
42 much attention due to their high sensitivity, good selectivity, short response time, and easy
43 monitoring^[16,17]. Various types of fluorescence chemosensors for detecting Fe^{3+} ions have been
44 reported, such as Schiff bases^[18], benzothiazole^[19], imidazole derivative^[20], coumarin derivatives^[21],
45 oxadiazole derivatives^[22], tetraphenylethylene-rhodamine^[23], cucurbit derivative^[24] and lots of
46 MOFs^[25,26]. Many MOFs fluorescent probes can also be used to detect $\text{Cr}_2\text{O}_7^{2-}$ ions, such as Ba-
47 MOFs^[27], Co-MOFs^[28], Cd-MOFs^[29,30], Re-MOFs(Re=Eu,Tb)^[31-34]. For toluene and xylene
48 fluorescence detection is relatively small. Only multifunctional nitrogen and sulfur doped
49 fluorescence carbon dots (N, S-CDs)^[35] can be used to detect toluene in aqueous solution, the
50 detection limit was low as $0.03\mu\text{M}$. As for nitrobenzene, the common fluorescent sensors are
51 $\text{Eu}^{3+}@\text{SOF}-1$ ^[36], Zn-MOFs^[37], Cd-MOFs^[38,39], UiO-66- NH_2 ^[40], etc. All of the above fluorescent
52 sensors have the advantages of high sensitivity, good selectivity, short response time and easy

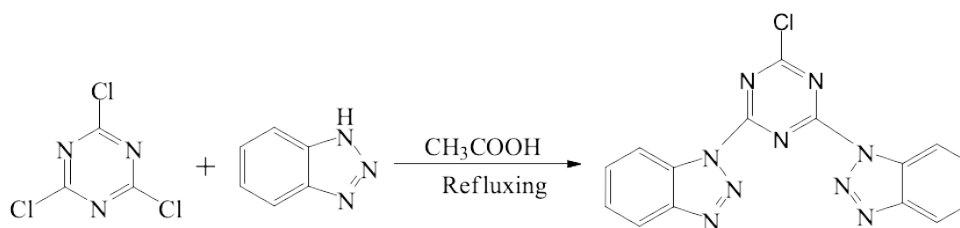
53 monitoring. However, single detection, complex synthesis and high price limit the application of
54 these fluorescent sensors.

55 In this work, a new complex, triazine nitrogen-rich derivative fluorescent probe, 1,1'-(6-
56 chloro-1,3,5-triazine-2,4-diyl)bis(1H-benzo[d][1,2,3]triazole)(**L**), has been prepared by reaction of
57 cyanuric chloride and 1,2,3-benzotriazole in glacial acetic acid. The compound **L** was investigated
58 for multiple fluorescence response to Fe^{3+} , $\text{Cr}_2\text{O}_7^{2-}$ ions, toluene, xylene and nitrobenzene. especially
59 it is first reported that the fluorescence intensity of compound **L** is enhanced when toluene and
60 xylene are added in DMF/ H_2O , respectively.

61 2| EXPERIMENTAL SECTION

62 2.1| Synthesis fluorescent probe compound **L**

63 1 mmol(0.1844 g) cyanuric chloride and 20 mL glacial acetic acid were added to a 50 mL round
64 bottom flask to dissolve it. And then 2 mmol(0.2663 g) 1,2,3-benzotriazole was added. The mixture
65 was stirred and refluxed immediately at 120 °C for 20 minutes, generating lots of white soild. Then,
66 the suspension was filtered and the product was washed several times with boiling water and
67 ethanol, and then dried in vacuum dryer at 80 °C for one day. The 0.3752 g white powder was
68 collected in 99.3% yield; 1,1'-(6-chloro-1,3,5-triazine-2,4-diyl)bis(1H-benzo[d][1,2,3]triazole) (**L**):
69 m.p. $\geq 330^\circ\text{C}$ (dec.); IR (KBr, cm^{-1}): 1598, 1537, 1485, 1462, 1333, 1295, 1233, 990, 753, 671;
70 ^1H NMR ($\text{DMSO}-d_6$, 500 MHz): δ 8.75 (d, $J = 5.0$ Hz, 2H, ArH), 8.31 (d, 3H, $J = 10.0$ Hz, ArH),
71 7.88-7.91 (m, 2H, ArH), 7.64-7.67 (m, 2H, ArH); ^{13}C NMR ($\text{DMSO}-d_6$, 125MHz) δ : 163.2, 146.6,
72 131.7, 131.0, 126.8, 120.7, 115.89, 79.7, 79.5, 79.2 cm^{-1} ; Anal. calcd for $\text{C}_{15}\text{H}_8\text{ClN}_9$ (Mr = 349.74):
73 C 51.51, N 36.04, H 2.31; found C 51.39, N 36.19, H 2.92.



75 **Scheme 1** The synthetic route of compound **L**

76 2.2| Fluorescence sensing experiments

77 2.2.1| Cations sensing

78 Because of the excellent fluorescence property of compound **L**, we were strongly interested to
79 explore the application of compound **L** for sensing metal ions in DMF/H₂O. A powder sample of
80 compound **L** was dissolved with sonification in 500 mL DMF/H₂O[V(DMF):V(H₂O)=24:1] to form
81 a solution of 1.3×10^{-3} mol/L. Add 0.1mL 20 different metal chloride (2.5×10^{-3} mol/L) to 2.9 mL the
82 solution of compound **L** at room temperature respectively. After full mixing for 10 s, the resultant
83 suspensions were then monitored by fluorescence spectroscopy and the fluorescence data were
84 collected under an excitation wavelength of 350 nm. Additionally, to confirm its selective
85 identification ability of Fe³⁺ among other ions, equal amounts of Fe³⁺ (1×10^{-3} M)solution was added
86 to the suspensions of compound **L** pretreated with other ions, respectively. and then the
87 fluorescence measurements were carried out. Respectively, different amounts of Fe³⁺ solution was
88 added into compound **L** aqueous to determine the relationship between the fluorescence intensity
89 and the concentration of compound **L**.

90 2.2.2| Anions sensing

91 Based on strong fluorescence properties of compound **L**, the fluorescence recognition anions were
92 further discussed. Add 0.1mL 27 different sodium salts (1×10^{-3} mol/L) to 2.9 mL the solution of
93 compound **L** at room temperature, respectively. After full mixing for 10 s, the resultant suspensions
94 were then monitored by fluorescence spectroscopy and the fluorescence data were collected under
95 an excitation wavelength of 350 nm. And then, to confirm its selective identification ability of
96 Cr₂O₇²⁻ among other anions, equal amounts of Cr₂O₇²⁻(1×10^{-3} M)solution was added to the
97 suspensions of compound **L** pretreated with other anions, respectively. and then the fluorescence
98 measurements were carried out. Respectively different amounts of Cr₂O₇²⁻ solution were added into
99 compound **L** aqueous to determine the relationship between the fluorescence intensity and the
100 concentration of compound **L**.

101 2.2.3|Organic solvent sensing

102 The effect of organic solvents on the fluorescence intensity of compound **L** were also studied. Add
103 0.1 mL 21 different organic solvents to 2.9 mL solution of compound **L** at room temperature,
104 respectively. After full mixing for 10 s, the resultant suspensions were then monitored by
105 fluorescence spectroscopy and the fluorescence data were collected under an excitation wavelength
106 of 350 nm. After that, to confirm its selective identification ability of toluene, xylene and
107 nitrobenzene among other organic solvents, equal amounts of toluene, xylene and nitrobenzene
108 solution were added to the suspensions of compound **L** pretreated with other organic solvents,
109 respectively.

110 **2.2.4| pH sensing**

111 The effect of pH on the fluorescence of compound **L** solution was also investigated. Add 0.1mL
112 different pH values aqueous solution to 2.9 mL solution of compound **L** at room temperature,
113 respectively. After full mixing for 10 s, the resultant suspensions were then monitored by
114 fluorescence spectroscopy and the fluorescence data which were collected under an excitation
115 wavelength of 350 nm.

116 **3| RESULTS AND DISCUSSION**

117 **3.1| Complexation ratio of compound **L** to Fe³⁺**

118 The Fe³⁺ ions exhibit superior fluorescence quenching effect on compound **L**. To explore the
119 detection effects of compound **L** in DMF/H₂O[V(DMF):V(H₂O)=24:1](1*10⁻⁴ M) as the
120 fluorescence probe of Fe³⁺ions, concentration-dependent experiments were further taken (Figure1a).
121 The fluorescence intensity of compound **L** gradually reduced with the increasing the proportion of
122 Fe³⁺ ions. The fluorescence intensity reaches the maximum when the ratio of compound **L** to Fe³⁺ is
123 9:1, and then decreases with the increase of the ratio of Fe³⁺ ions. The Job's curve was given
124 according to the fluorescence concentration curve of compound **L** and Fe³⁺ ions (Figure 1b). The
125 results showed that the molar fraction of [Fe³⁺]/[L+Fe³⁺] was 0.1 when the curve has inflection
126 point, demonstrating 2:1 binding stoichiometry ration for **L**+Fe³⁺.

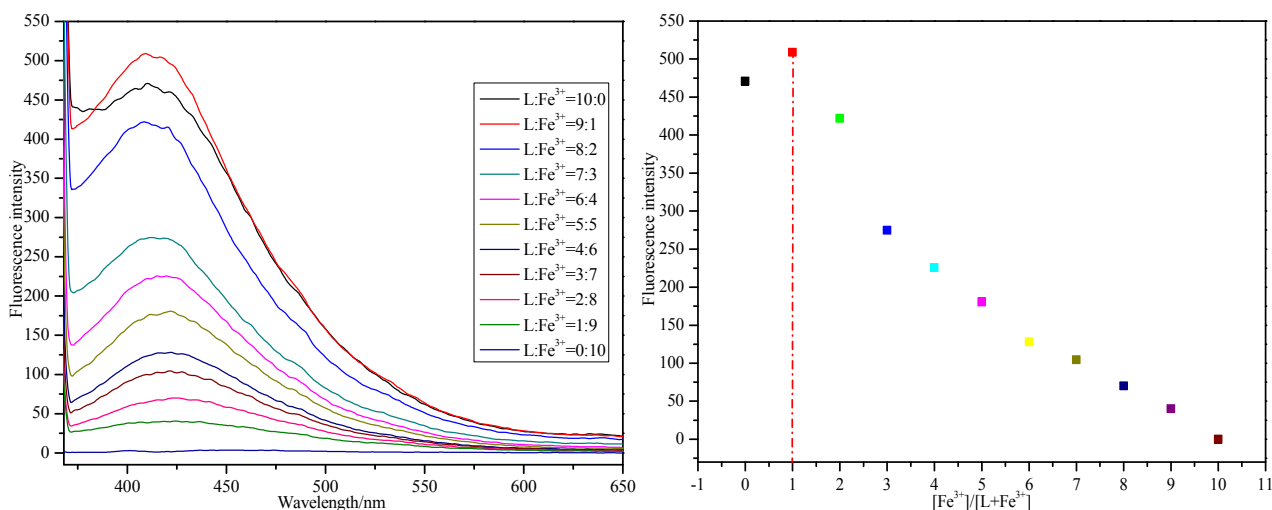


FIGURE 1 (a) Fluorescence spectra of different proportions of **L** and Fe^{3+} ions at the same concentration ($\lambda_{\text{ex}}=350$ nm, slit = 10 nm), $[\text{L}]=1 \times 10^{-3}$ M, $[\text{Fe}^{3+}]=1 \times 10^{-3}$ M; (b) The Job's plot of **L** with Fe^{3+} ions.

3.2| Selective sensing of Fe^{3+} ions

As shown in Figure 2, the fluorescence intensity of compound **L** at 409 nm reduced obviously when metal ions (Li^+ , Na^+ , K^+ , Cu^+ , Mg^{2+} , Zn^{2+} , Ba^{2+} , Ca^{2+} , Cu^{2+} , Mn^{2+} , Ni^{2+} , Co^{2+} , Pb^{2+} , Sn^{2+} , Hg^{2+} , Cd^{2+} , Sb^{3+} , Sr^{3+} , Cr^{3+} and Fe^{3+} ions) were added, respectively. Compared with other metal ions, after addition of Fe^{3+} ions, the fluorescence intensity at 409 nm was quenched with a quenching ratio of 42%, which enabled the “turn-off” detection of Fe^{3+} ions.

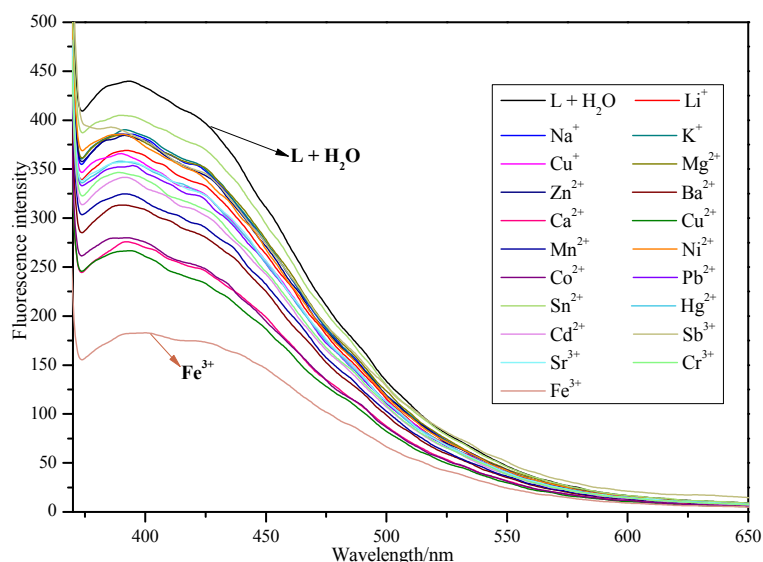
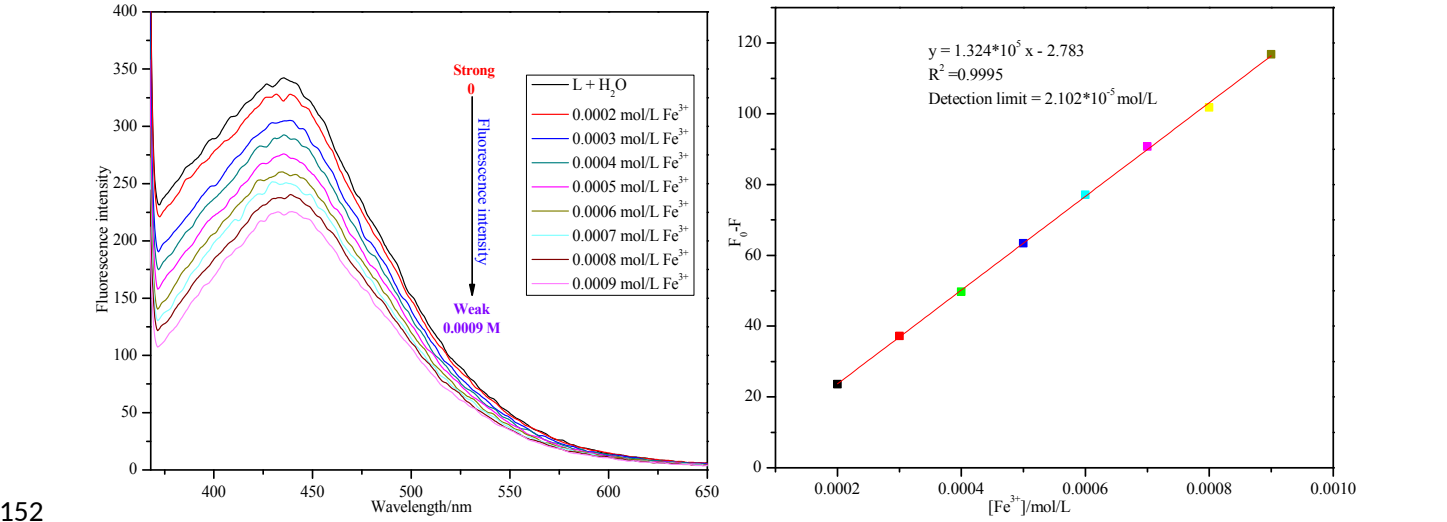


FIGURE 2 Fluorescence change of **L** (DMF/ H_2O) in different metal chloride aqueous solution, **L** = 2.9 mL, 1.3×10^{-3} M, metal chloride = 0.1 mL, 2.5×10^{-3} mol/L, $\lambda_{\text{ex}} = 350$ nm, slit = 10 nm.

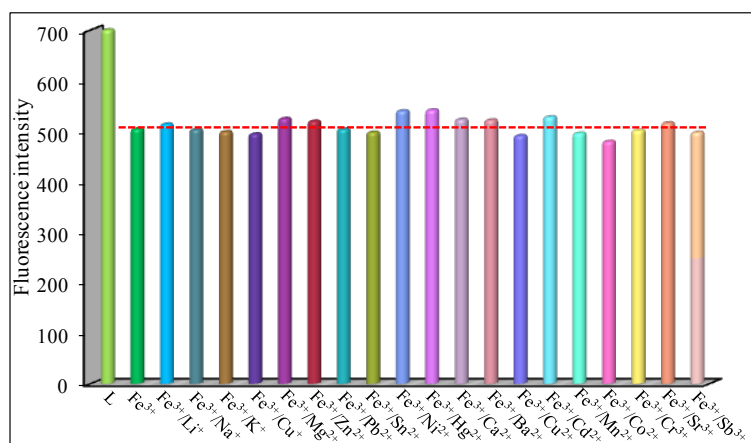
The experiment of Fe^{3+} ions concentration showed that the fluorescence intensity of compound **L** reduced with the increase of the concentration of Fe^{3+} ions (Figure 3a). The fluorescence intensity

141 of compound **L** shows a highly broad linear relationship with the concentration of Fe^{3+} ion from
 142 2×10^{-4} to 9×10^{-4} M expressed as an equation of $y = 1.324 \times 10^5 x - 2.783$ and $R^2 = 0.9995$. where y is
 143 the ratio of $(F-F_0)$ and x is the concentration of Fe^{3+} ions. According to the fluorescence intensity of
 144 compound **L**, different concentration of Fe^{3+} ions, Benesi-Hildebrand equation, the detection limit
 145 of Fe^{3+} ions in compound **L**(DMF/ H_2O) is calculated to be 2.10×10^{-5} mol/L(Figure3b). In addition,
 146 the quenching efficiency can be rationalized by the Stern–Volmer(SV) equation, $F_0/F = 1 + K_{\text{SV}}[\text{M}]$,
 147 where F_0 and F are the relative fluorescence intensity before and after adding Fe^{3+} ions, $[\text{M}]$ is the
 148 molar concentration of the Fe^{3+} ions, and K_{SV} (M^{-1}) is the Stern–Volmer quenching constant. The
 149 $K_{\text{SV}}(\text{Fe}^{3+})$ value is calculated as 470.00 M^{-1} which indicated that Fe^{3+} have a strong enhancement
 150 effect on the fluorescence of compound **L**. Under the same conditions, the quenching constants of
 151 other metals are shown(Table S1).



153 **FIGURE 3** (a)Fluorescence change of **L** (DMF/ H_2O) in different concentrations of Fe^{3+} ions, **L** = 2.9 mL, 1.3×10^{-3} mol/L, $[\text{Fe}^{3+}] = 0.1 \text{ mL}$, $2 \times 10^{-4} \sim 9 \times 10^{-4}$ mol/L, $\lambda_{\text{ex}} = 350 \text{ nm}$, slit = 10nm; (b) Detection limit of Fe^{3+} ions.

155 The interference of other metal ions on Fe^{3+} ions was also investigated, respectively(Figure 4).
 156 For Fe^{3+} ions, most metal ions have little interference with Fe^{3+} in the DMF/ H_2O of compound **L**.
 157 Therefore, compound **L** exhibited selectivity and specificity for detection of Fe^{3+} in the presence of
 158 these other metal ions.

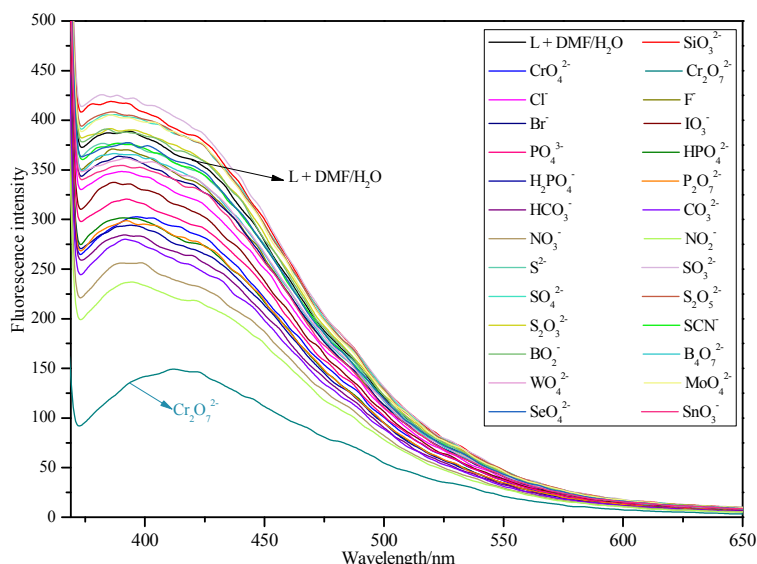


159

160 **FIGURE 4** The influence of metal ions interference on the fluorescence recognition of Fe^{3+} by compound
 161 **L**(DMF/ H_2O), **L** = 2.8 mL, 1.3×10^{-3} mol/L, metal ions = 0.1mL, 1×10^{-3} mol/L, $\lambda_{\text{ex}}=350\text{ nm}$, slit =10 nm.

162 3.3| Selective sensing of $\text{Cr}_2\text{O}_7^{2-}$ ions

163 The fluorescence properties are recorded and listed in Figure 5($\lambda_{\text{ex}}=350\text{ nm}$). The fluorescence
 164 intensity changed slightly when 26 anions (F^- , Cl^- , Br^- , IO_3^- , H_2PO_4^- , HPO_4^{2-} , PO_4^{3-} , $\text{P}_2\text{O}_7^{2-}$, HCO_3^- ,
 165 CO_3^{2-} , NO_2^- , NO_3^- , S^{2-} , SO_3^{2-} , $\text{S}_2\text{O}_3^{2-}$, SO_4^{2-} , $\text{S}_2\text{O}_5^{2-}$, BO_2^- , $\text{B}_4\text{O}_7^{2-}$, SCN^- , CrO_4^{2-} , MnO_4^- , SnO_3^- , SeO_4^{2-} ,
 166 MoO_4^{2-} and WO_4^{2-}) were added, respectively. Apparently, the fluorescence intensity of compound **L**
 167 was reduced at 414 nm obviously only by adding $\text{Cr}_2\text{O}_7^{2-}$ ions, which enabled the “turn-off”
 168 detection of $\text{Cr}_2\text{O}_7^{2-}$ ions.

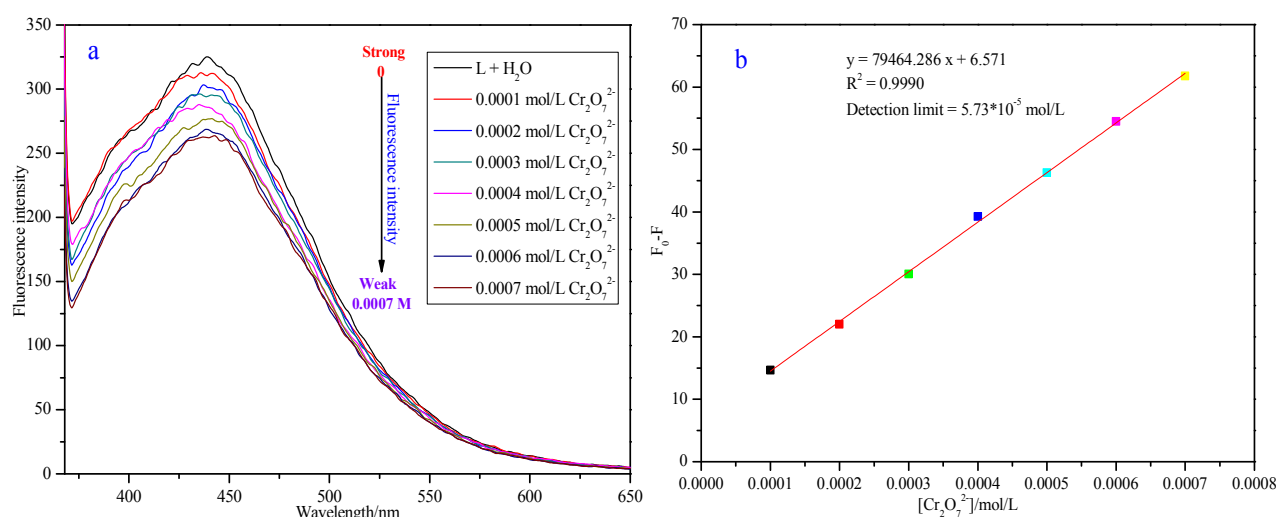


169

170 **FIGURE 5** Fluorescence change of **L**(DMF/ H_2O) in different anions solution, **L** = 1.3×10^{-3} mol/L, anions =
 171 0.1mL, 1×10^{-3} mol/L, $\lambda_{\text{ex}}=350\text{ nm}$, slit =10 nm.

172 The results show that with the addition of different concentrations $\text{Cr}_2\text{O}_7^{2-}$ ions, the
 173 fluorescence intensity of compound **L** gradually reduces and shows a highly broad linear

relationship with the concentration of $\text{Cr}_2\text{O}_7^{2-}$ ions from 1×10^{-4} to 7×10^{-4} M expressed as an equation of $y = 79464x + 6.571$ and $R^2 = 0.9990$, where y is the ratio of F_0/F and x is the concentration of $\text{Cr}_2\text{O}_7^{2-}$ ions (Figure 6a). According to the fluorescence intensity of compound **L**, different concentration of $\text{Cr}_2\text{O}_7^{2-}$ ions and Benesi-Hildebrand equation, the detection limit of $\text{Cr}_2\text{O}_7^{2-}$ ions in compound **L** (DMF/ H_2O) is calculated to be 5.73×10^{-5} mol/L (Figure 6b). Further, the quenching efficiency can be rationalized by the Stern–Volmer (SV) equation, $F_0/F = 1 + K_{\text{SV}}[M]$, where F_0 and F are the relative fluorescence intensity before and after adding $\text{Cr}_2\text{O}_7^{2-}$ ions, $[M]$ is the molar concentration of the $\text{Cr}_2\text{O}_7^{2-}$ ions, and K_{SV} (M^{-1}) is the Stern–Volmer quenching constant. The $K_{\text{SV}}(\text{Cr}_2\text{O}_7^{2-})$ value is calculated as 359.94 M^{-1} , suggesting a strong quenching effect on fluorescence. Under the same conditions, the quenching constants of other anions are shown (Table S2).



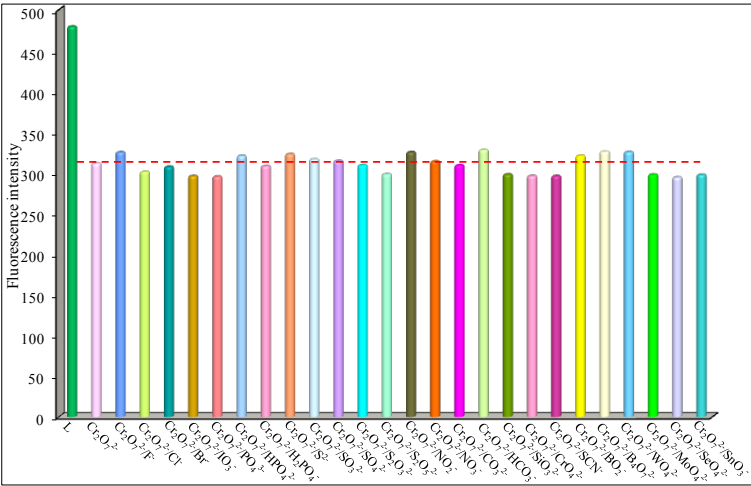
185

186 **FIGURE6** (a) Fluorescence change of **L** (DMF/ H_2O) in different concentrations of $\text{Cr}_2\text{O}_7^{2-}$ ions, **L** = 2.9 mL, 1.3×10^{-3} mol/L, $[\text{Cr}_2\text{O}_7^{2-}] = 0.1 \text{ mL}$, $1 \times 10^{-4} \sim 7 \times 10^{-4}$ mol/L, $\lambda_{\text{ex}} = 350 \text{ nm}$, slit = 10 nm; (b) Detection limit of $\text{Cr}_2\text{O}_7^{2-}$ ions.

189 The interference of other anions on $\text{Cr}_2\text{O}_7^{2-}$ ions was also discussed, respectively. The interference of 25 anions on the $\text{Cr}_2\text{O}_7^{2-}$ ions are shown in Figure 7. These anions did not induce a significant decrease in the fluorescence of $\text{Cr}_2\text{O}_7^{2-}$ ions in compound **L** (DMF/ H_2O). Only a few anions cause a slight decrease in the fluorescence intensity of $\text{Cr}_2\text{O}_7^{2-}$ ions in compound **L** from the histogram analysis. However the whole fluorescence intensity is lower than without adding any anions. It demonstrated that compound **L** can detect $\text{Cr}_2\text{O}_7^{2-}$ ions in the presence of these other

194

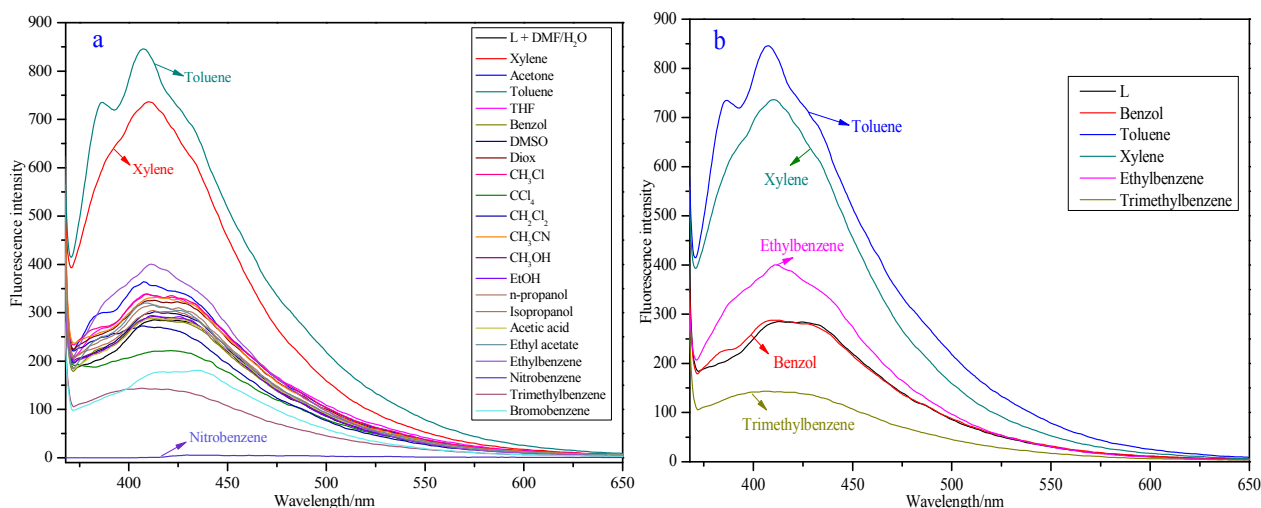
195 anions respectively.



197 **FIGURE 7** The influence of anions interference on the fluorescence recognition of Cr₂O₇²⁻ ions by compound
198 **L**(DMF/H₂O), **L** = 2.8 mL, 1.3*10⁻³ mol/L, anions = 0.1mL, 1*10⁻³ mol/L, λ_{ex}=350nm, slit =10 nm.

199 **3.4| Selective sensing of toluene, xylene and nitrobenzene**

200 The fluorescence properties are recorded and listed in Figure 8a (λ_{ex}=350 nm). The fluorescence
201 intensity of compound **L** were decreased and enhanced at 410 nm when 21 organic
202 solvents(CH₃OH, EtOH, CH₂Cl₂, CHCl₃, CCl₄,THF, DMSO, Diox, CH₃CN, CH₃COOH, acetone,
203 benzol, toluene, xylene, trimethylbenzene, ethylbenzene, n-propanol, isopropanol, ethyl acetate,
204 bromobenzene and nitrobenzene) were added, respectively. Compared with other solvents, the
205 fluorescence intensity of compound **L** were obviously enhanced when toluene and xylene were
206 added, respectively. The fluorescence enhancement are 2.5 and 3 times that of compound **L**,
207 respectively, which enabled the “turn-on” detection of toluene and xylene. Interestingly, only
208 toluene, xylene and ethylbenzene can enhance the fluorescence of compounds **L** in the series of
209 benzene, toluene, xylene, trimethylbenzene and ethylbenzene homologues, especially toluene and
210 xylene(Figure 8b). On the contrary, the fluorescence intensity of compound **L** was quenched with a
211 quenching ratio of 99%, which enabled the “turn-off” detection of nitrobenzene.

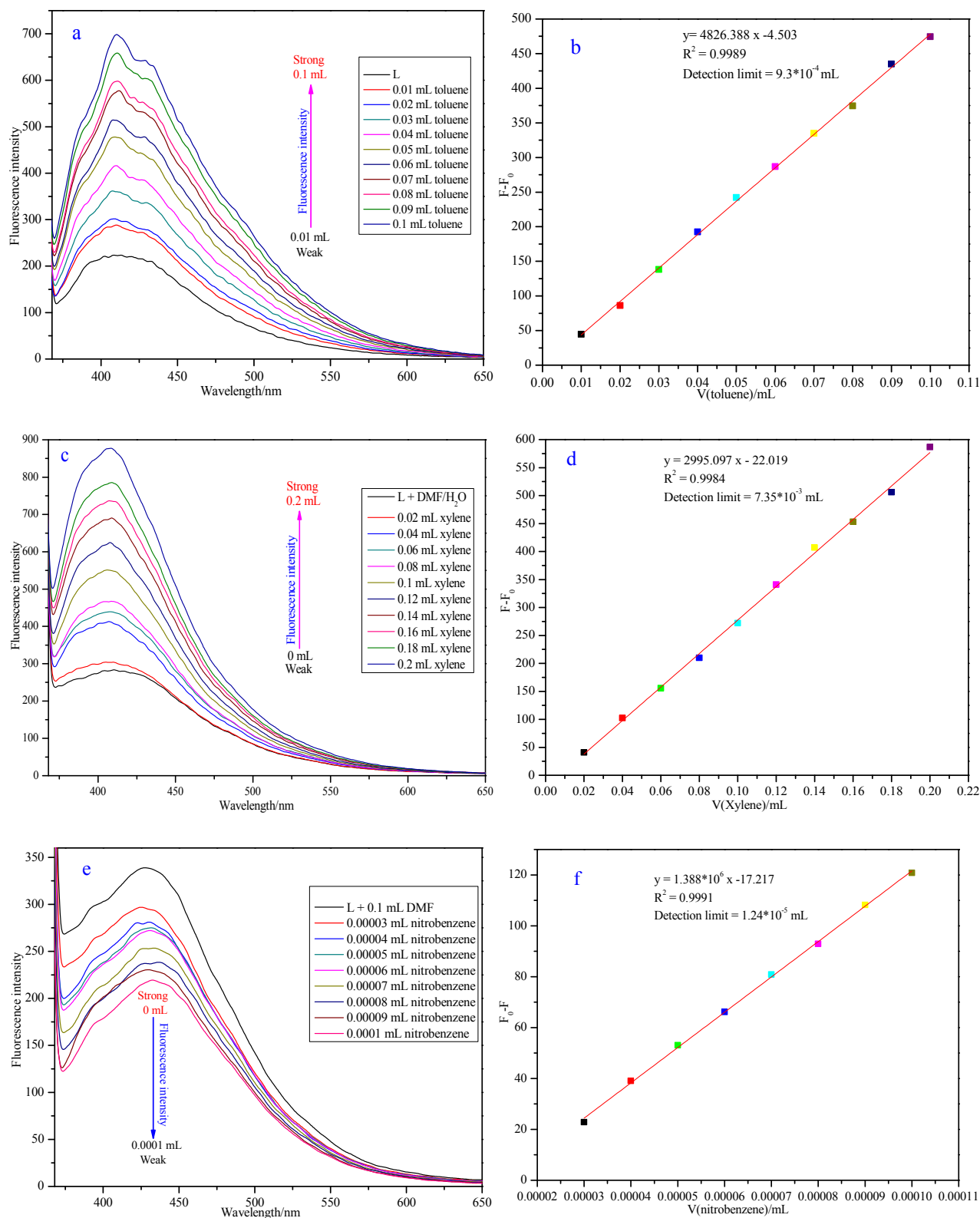


212

213 **FIGURE 8(a)** Fluorescence changes of compound **L** in different organic solvents, **L** = 2.9 mL, 1.3×10^{-3} mol/L,
 214 organic solvents = 0.1 mL, λ_{ex} = 350 nm, slit = 10 nm; (b) Fluorescence changes of benzene homologues in
 215 compound **L** in DMF/H₂O.

216 The experimental results show that with the addition of different volumes of toluene and
 217 xylene, respectively (Figure 9a,c), the fluorescence intensity of compound **L** gradually enhances and
 218 shows a highly broad linear relationship with the volume of toluene from 0.01 to 0.1 mL expressed
 219 as an equation of $y = 4826.388x - 4.503$ and $R^2 = 0.9989$, and linear relationship with the volume
 220 of xylene from 0.02 to 0.2 mL expressed as an equation of $y = 2995.097x - 22.019$ and $R^2 =$
 221 0.9984 , where y is the ratio of F/F_0 and x is the volume of xylene (Figure 9b,d). According to the
 222 fluorescence intensity of compound **L**, different volumes of toluene, xylene and Benesi-Hildebrand
 223 equation, the detection limit of toluene in compound **L** solution are calculated to be 9.3×10^{-4} mL
 224 and 7.35×10^{-3} mL. Further, the quenching efficiency can be rationalized by the Stern–Volmer (SV)
 225 equation, $F_0/F = 1 + K_{\text{SV}}[V]$, where F_0 and F are the relative fluorescence intensity before and after
 226 adding toluene(xylene), $[V]$ is the volume of the toluene(xylene), and K_{SV} (V^{-1}) is the Stern–Volmer
 227 quenching constant. The K_{SV} (toluene, xylene) values are calculated as -11.05 mL^{-1} and -6.23 mL^{-1} ,
 228 suggesting a strong enhancing effect on fluorescence. On the contrary, the fluorescence intensity of
 229 compound **L** gradually decreases and shows a highly broad linear relationship with the volume of
 230 nitrobenzene from 0.00003 to 0.0001 mL expressed as an equation of $y = 1.388 \times 10^6x - 17.217$ and
 231 $R^2 = 0.9991$, where y is the ratio of F/F_0 and x is the volume of nitrobenzene (Fig. 9f). According to
 232 the fluorescence intensity of compound **L**, different volumes of nitrobenzene and Benesi-

233 Hildebrand equation, the detection limit of nitrobenzene in compound **L** solution are calculated to
 234 be 1.24×10^{-5} mL. The $K_{SV}(\text{nitrobenzene})$ value are calculated as $3.62 \times 10^3 \text{ mL}^{-1}$, suggesting a strong
 235 quenching effect on fluorescence. Under the same conditions, the quenching constants of other
 236 organic solvents are shown (Table S3).



240 **FIGURE 9** (a) Fluorescence changes of compound **L** in different volumes of toluene, **L** = 2.9 mL, 1.3×10^{-3}

275 3.6| Mechanism of sensing

276 The competition between absorption and emission spectra is one of the causes of fluorescence
277 quenching^[41]. For Fe^{3+} and $\text{Cr}_2\text{O}_7^{2-}$ ions, there are partial overlap between the absorption spectrum of
278 Fe^{3+} and $\text{Cr}_2\text{O}_7^{2-}$ ions with the emission spectrum of **L**, which were competitive adsorption between
279 Fe^{3+} , $\text{Cr}_2\text{O}_7^{2-}$ ions and **L**(Figure S4). According to Fe^{3+} and $\text{Cr}_2\text{O}_7^{2-}$ ions fluorescence experiments,
280 the fluorescence of compound **L** was not completely quenched when 0.1mL Fe^{3+} and $\text{Cr}_2\text{O}_7^{2-}$
281 ions(1×10^{-3} mol/L) were added, respectively. In addition, there is a larger overlap between the
282 absorption spectra of nitrobenzene and the emission spectra of compound **L** from 350nm to 427 nm.
283 In the competition, the absorption of nitrobenzene is obviously stronger than the emission of
284 compound **L**. Therefore, the nitrobenzene has a strong fluorescence quenching effect on compound
285 **L**. In contrast, the toluene and xylene have no absorption peaks at 350-500nm in the UV spectrum.
286 There is not evidence for competitive adsorption between toluene, xylene and compound **L**,
287 respectively. It could be inferred that the toluene and xylene could induce the aggregation of
288 compound **L** in DMF solution, thus resulting in an enhanced fluorescence intensity.

289 3.7|Application to the determination of Fe^{3+} in water samples, vegetables and the 290 determination of toluene and xylene in gasoline

291 The samples were taken from the Yellow River, the Park Lake and the tap water. The Yellow River
292 and the Park Lake must be purified by centrifugation for 10 minutes at 5000 rpm to remove solid
293 impurities. The tap water is boiled for 5 minutes to remove the HClO from the water. Fresh
294 vegetables are bought from the vegetable market and are ground, nitrated, filtered, centrifuged and
295 pH adjusted to neutral. Add 0.1 mL samples directly to compound **L** DMF/ H_2O solution without
296 any other treatment before test analysis. The concentration of Fe^{3+} ions in samples were calculated
297 by Stern–Volmer(SV) equation and $y = 1.324 \times 10^5 x - 2.783$ were shown in Table 1. The error
298 range of Fe^{3+} ions in water samples and vegetables were about 0.11-0.42 by calculation. The
299 standard solutin to the error is found to be less than 0.11 by solving two curve equations. In general,
300 the iron mass in cabbage, potato and spinach are 0~5mg, 0~1mg and 0-2.5 mg/100 g, respectively.
301 According to the analysis and calculation, the mass of iron is 1.7-2.1 mg, 1.3-1.7 mg and 1.0-1.3

mg, respectively. In a sense, the compound **L** can be used as a fluorescence probe to measure the molarity of Fe³⁺ ion conveniently.

Table 1 Detection of Fe³⁺ ion concentration in water samples and vegetables by fluorescence of compound **L**^a

Samples	F ₀	F	[Fe ³⁺]/10 ⁻⁴ mol/L		Error
			F ₀ /F ^b	Y ^c	
Standard Solution	342.30	275.86	5.12	5.23	±0.11
Yellow River	342.30	323.57	1.23	1.62	±0.39
Park Lake	342.30	324.08	1.20	1.59	±0.39
Tap Water	342.30	320.70	1.43	1.84	±0.41
Cabbage	342.30	315.23	1.83	2.25	±0.42
Potatoes	342.30	321.52	1.37	1.77	±0.40
Spinach	342.30	326.46	1.03	1.41	±0.38

^a(L =2.9 mL, 1.3*10⁻³ mol/L; sample = 0.1 mL; λ_{ex}=350 nm, slit =10 nm); ^bF₀/F=1+K_{SV}[Fe³⁺]; ^cY = 1.324*10⁵ x – 2.783.

The gasoline(92#), diesel(0#) and engine oil are purchased from gas stations. Add different volumes samples directly to compound **L** DMF/H₂O solution without any other treatment before test analysis. It found that toluene or xylene can be distinguished from gasoline, diesel and engine oil by the fluorescence curve of compound **L**(Figure S5). The results show that toluene is one of the aromaticity found in gasoline(92#), and there are isomers of xylene (except ethylbenzene) in diesel oil and engine oil. In addition, The volume of toluene and xylene in samples were calculated by Stern–Volmer(SV) equation and y(toluene) = 4826.388 x – 4.503, y(xylene) =2995.097 x -22.019 were shown in Table 2. The standard solutin to the error is found to be less than 0.001 by solving two curve equations, the error range of samples were about 0.022 and 0.010-0.011 by calculation. In a sense, the compound **L** can be used as a fluorescence probe conveniently to toluene and xylene in gasoline, diesel and engine oil.

Table 2 Detection of toluene and xylene volume in gasoline, diesel and engine oil by fluorescence of compound **L**^a

Samples	F ₀	F	V _{toluene} /mL		V _{xylene} /mL		Error
			F ₀ /F ^b	Y ^c	F ₀ /F ^d	Y ^e	
toluene	283.40	416.14	0.029	0.028	–	–	±0.001
xylene	283.40	412.81	–	–	0.050	0.051	±0.001
gasoline(92#)	283.40	569.34	–	–	0.081	0.103	±0.022
diesel(0#)	283.40	533.95	0.042	0.052	–	–	±0.010

	Engine oil	283.40	547.37	0.044	0.055	—	—	±0.011
--	------------	--------	--------	-------	-------	---	---	--------

^a(L = 2.9 mL, 1.3 × 10⁻³ mol/L; sample = 0.1 mL; λ_{ex} = 350 nm, slit = 10 nm); ^bF₀/F = 1 + K_{SV} V_{toluene}; ^cY = 4826.388 x - 4.503;
^dF₀/F = 1 + K_{SV} V_{xylene}; ^eY = 2995.09 x - 22.019.

4| Conclusions

In conclusion, A multiple fluorescent sensor was developed for the sensitive and selective detection of Fe³⁺, Cr₂O₇²⁻ ions in aqueous solution, and probe detection of toluene, xylene and nitrobenzene in DMF solution. Compared with the reported chemical fluorescence sensors, the compound **L** is able to detect toluene and xylene, which are due to the enhancement of fluorescence of the compound **L** by toluene and xylene. The chemical fluorescence sensors for the detection of toluene and xylene are rarely reported. The compound **L** has been applied to the detection of Fe³⁺ in water samples and vegetables, and the good results have been obtained. Of course, the compound **L** is also used as a chemical fluorescent sensor to detect toluene and xylene in gasoline, diesel and engine oil, and the good results have been obtained.

ACKNOWLEDGEMENTS

This work was supported financially by the National Natural Science Foundation of China (No.51964041), the Natural Science Foundation of Inner Mongolia (No. 2018BS02009).

REFERENCES

- [1] Sun X, Yao S, Yu C, et al. An ultrastable Zr-MOF for fast capture and highly luminescence detection of Cr₂O₇²⁻ simultaneously in an aqueous phase. *J. Mater. Chem. A*. 2018; 6: 6363–6369.
- [2] Ding Y, Zhu W H, Xie Y. Development of ion chemosensors based on porphyrin analogues. *Chem. Rev.* 2016; 117:2203–2256.
- [3] Zhang Q, Lei M, Yan H, et al. A water-stable 3D luminescent metal-organic framework based on heterometallic [Eu^{III}₆Zn^{II}] clusters showing highly sensitive, selective, and reversible detection of ronidazole. *Inorg. Chem.* 2017;56:7610–7614.
- [4] Zhou W, Saran R, Liu J. Metal Sensing by DNA. *Chem. Rev.* 2017;117:8272–8325.
- [5] Liu W, Wang Y. Bai Z, et al. Hydrolytically Stable Luminescent Cationic Metal Organic Framework for Highly Sensitive and Selective Sensing of Chromate Anions in Natural Water Systems. *ACS Appl. Mater. Interfaces*, 2017; 9:16448–16457.

346 [6] Cao CS, Shi Y, Xu H, et al. A multifunctional MOF as a recyclable catalyst for the fixation of CO₂ with
 347 aziridines or epoxides and as a luminescent probe of Cr(VI). *Dalton Trans.* 2018; 47:4545–4553.

348 [7] Desai AV, Manna B, Karmakar A, et al. A Water–Stable Cationic Metal–Organic Framework as a Dual
 349 Adsorbent of Oxoanion Pollutants. *Angew. Chem. Int. Ed.* 2016;55:7811–7815.

350 [8] Zhao L, Zhang J, Wang J, et al. Structural diversity, gas sorption properties, luminescent sensing of three
 351 Cd(II) complexes based on 3, 5-Di(2', 5-dicarboxylphenyl)pyridine. *J. Solid State Chem.* 2018;268: 1–8.

352 [9] Yang Y, Qiu F, Xu C et al. A multifunctional Eu-CP as a recyclable luminescent probe for the highly sensitive
 353 detection of Fe³⁺/Fe²⁺, Cr₂O₇²⁻, and nitroaromatic explosives. *Dalton Trans.* 2018;47:7480–7486.

354 [10] Wolkoff P, Nielsen GD. Organic compounds in indoor air—their relevance for perceived indoor air quality.
 355 *Atmos. Environ.* 2001;35: 4407–4417.

356 [11] Yücel M, Takagi M, Walterfang M, et al. Toluene misuse and long-term harms: a systematic review of the
 357 neuropsychological and neuroimaging literature. *Neurosci. Biobehav. Rev.* 2008;32:910–926.

358 [12] Thomas SW, Joly GD, Swager T M. Chemical Sensors Based on Amplifying Fluorescent Conjugated
 359 Polymers. *Chem. Soc. Rev.* 2007;36:1339–1386.

360 [13] Ignacio LG, Natalia C, Isabel AJ, et al. Slurry sampling for the determination of silver and gold in soils and
 361 sediments using electrothermal atomic absorption spectrometry. *Spectrochim. Acta. B.* 2003;58:1715–1721.

362 [14] Mohadesi A, Taher MA. Stripping voltammetric determination of silver(I) at carbon paste electrode modified
 363 with 3-amino-2-mercapto quinazolin-4(3H)-one. *Talanta.* 2007;71: 615–619.

364 [15] Ndung'u K, Ranville MA, Franks RP, et al. On-line determination of silver in natural waters by inductively-
 365 coupled plasma mass spectrometry: influence of organic matter. *Mar. Chem.* 2006;98:109–120.

366 [16] Sedgwick AC, Wu L, Han HH, et al. Excited-state intramolecular proton-transfer (ESIPT) based fluorescence
 367 sensors and imaging agents. *Chem. Soc. Rev.* 2018;47:8842–8880.

368 [17] Park SH, Kwon N, Lee JH, et al. Synthetic ratiometric fluorescent probes for detection of ions. *Chem. Soc.*
 369 *Rev.* 2020;49:143–79.

370 [18] Ju P, Su Q, Liu Z. A salen-based covalent organic polymer as highly selective and sensitive fluorescent
 371 sensor for detection of Al³⁺, Fe³⁺ and Cu²⁺ ions, *J. Mater. Sci.* 2019;54: 851–861.

372 [19] Gong X, Ding X, Jiang N, et al. Benzothiazole-based fluorescence chemosensors for rapid recognition and
 373 “turn-off” fluorescence detection of Fe³⁺ ions in aqueous solution and in living cells. *Microchem. J.* 2020;152:
 374 104351.

375 [20] Zhao B, Liu T, Fang Y, et al. A new selective chemosensor based on phenanthro[9,10-d]imidazole-coumarin
376 with sequential “on-off-on” fluorescence response to Fe^{3+} and phosphate anions and its application in live cell.
377 *Sens. Actuat. B-Chem.* 2017;246:370–379.

378 [21] Wang L, Li W, Zhi W. A new coumarin Schiff based fluorescent-colorimetric chemosensor for dual
379 monitoring of Zn^{2+} , and Fe^{3+} in different solutions: an application to bio-imaging. *Sens. Actuat. B-Chem.* 2018;26:
380 243–254.

381 [22] Chen JM, Zeng J, Zhang Z, et al. A Novel Colorimetric Fluorescent Probe for Fe^{3+} Based on
382 Tetraphenylethylene-rhodamine. *Chin. J. Anal. Chem.* 2019;47:19139–19146.

383 [23] Gong X, Zhang HY, Jiang N. Oxadiazole-based ‘on-off’ fluorescence chemosensor for rapid recognition and
384 detection of Fe^{2+} and Fe^{3+} in aqueous solution and in living cells. *Microchem. J.* 2019;145:435–443.

385 [24] Zhang W, Luo Y, Zhou Y, et al. A highly selective fluorescent chemosensor probe for detection of Fe^{3+} and
386 Ag^+ based on supramolecular assembly of cucurbit[10]uril with a pyrene derivative. *Dyes Pigm.*
387 2020;176:108235. [25] Chen X B, Qi CX, Li H, et al. Highly sensitive and selective Fe^{3+} detection by a water-
388 stable Tb^{3+} -doped nickel coordination polymer-based turn-off fluorescence sensor. *J. Solid State Chem.*
389 2020;281:121030.

390 [26] Feng DD, Tang J, Yang J, et al. A multiresponsive luminescent probe of antibiotics, pesticides, Fe^{3+} and
391 ascorbic acid with a Cadmium(II) metal-organic framework. *J. Mol. Struct.* 2020;1221:128841.

392 [27] Li FF, Zhu ML, Lu LP, et al. A novel monocapped square-antiprismatic Ba(II) coordination polymer:
393 a design for dual-responsive fluorescent chemosensor for $\text{Cr}_2\text{O}_7^{2-}$ and Fe(III). *J. Solid State Chem.* 2020; 290:
394 121582.

395 [28] Liu GC, Li Y, Chi J, et al. Multi-functional fluorescent responses of cobalt complexes derived from
396 functionalized amide-bridged ligand. *Dyes Pigm.* 2020;174:108064.

397 [29] Qin BW, Zhang XY, Zhang JP. A stable multifunctional cadmium-organic framework based on 2D stacked
398 layers: Effective gas adsorption, and excellent detection of Cr^{3+} , CrO_4^{2-} , and $\text{Cr}_2\text{O}_7^{2-}$. *Dyes Pigm.* 2020;174:
399 108011.

400 [30] Zhu H, Li YH, Xiao QQ, et al. Three luminescent Cd(II) coordination polymers containing aromatic
401 dicarboxylate and flexible bis(benzimidazole) ligands as highly sensitive and selective sensors for detection of
402 $\text{Cr}_2\text{O}_7^{2-}$ oxoanions in water. *Polyhedron.* 2020;187:114648.

[31] Yang Y, Qiu F, Xu C, et al. A multifunctional Eu-CP as a recyclable luminescent probe for the highly sensitive detection of $\text{Fe}^{3+}/\text{Fe}^{2+}$, $\text{Cr}_2\text{O}_7^{2-}$, and nitroaromatic explosives. *Dalton Trans.* 2018;47:7480–7486.

[32] Wang YN, Wang SD, Wang WJ, et al. Ln-CPs constructed from unsymmetrical tetracarboxylic acid ligand: Tunable white-light emission and highly sensitive detection of CrO_4^{2-} , $\text{Cr}_2\text{O}_7^{2-}$, MnO_4^- in water. *Spectrochim. Acta A.* 2020;229:117915.

[33] Gao LJ, Jiao CX, Chai HM, et al. A highly sensitive multifunctional Eu-MOF sensor with pentacarboxylate for fluorescence detecting acetone, Cu^{2+} and $\text{Cr}_2\text{O}_7^{2-}$, and electrochemical detection of TNP. *J. Solid State Chem.* 2020;284:121199.

[34] Guo F, Chu ZP, Zhao MH, et al. A dual-responsive luminescent Tb^{III} -organic framework with high water stability for selective sensing of Fe^{3+} and $\text{Cr}_2\text{O}_7^{2-}$ in water systems. *Inorg. Chem. Commun.* 2019;104: 71–77.

[35] Wang JL, Wu ZL, Chen SH, et al. A novel multifunctional fluorescent sensor based on N/S co-doped carbon dots for detecting Cr(VI) and toluene. *Microchem. J.* 2019;151:104246.

[36] Jiang DY, Fang HF, Li G, et al. A responsive supramolecular-organic framework: Functionalization with organic laser dye and lanthanide ions for sensing of nitrobenzene. *J. Solid State Chem.* 2020; 284: 121171.

[37] Duan XD, Ge FY, Zheng HG. Two bifunctional photoluminescent Zn (II) coordination polymers for detection of Fe^{3+} ion and nitrobenzene. *Inorg. Chem. Commun.* 2019;107:107479.

[38] Shi M, Yang J, Liu YY, et al. Four coordination polymers based on 1,4,8,11-tetrazacyclotetradecane- $\text{N}_4\text{N}'_4\text{N}''_4\text{N}'''_4$ -tetra-methylene-benzoic acid: Syntheses, structures, and selective luminescence sensing of iron(III) ions, dichromate anions, and nitrobenzene. *Dyes Pigm.* 2016;129:109–120.

[39] Yousaf A, Xu N, Arif AM, et al. A triazine-based metal-organic framework with solvatochromic behaviour and selectively sensitive photoluminescent detection of nitrobenzene and Cu^{2+} ions. *Dyes Pigm.* 2019; 163:159–167.

[40] Vellingiri K, Boukhvalov DW, Pandey SK, et al. Luminescent metal-organic frameworks for the detection of nitrobenzene in aqueous media. *Sens. Actuat. B-Chem.* 2017; 245:305–313.

429 [41] Wang XQ, Feng DD, Tang J, et al. A water-stable zinc(ii)–organic framework as a multiresponsive
430 luminescent sensor for toxic heavy metal cations, oxyanions and organochlorine pesticides in aqueous
431 solution. *Dalton Trans.* 2019;48:16776–16785.